Available online at www.sciencedirect.com

Journal of Photochemistry and Photobiology A: Chemistry 170 (2005) 61–67

Journal of Photochemistry and Photobiology A:Chemistry

www.elsevier.com/locate/jphotochem

Photoinduced halophenol formation in the presence of iron(III) species or cadmium sulfide

P. Calza, V. Maurino, C. Minero, E. Pelizzetti*, M. Sega, M. Vincenti

Dipartimento di Chimica Analitica, Università di Torino, via P.Giuria 5, 10125 Torino, Italy

Received 31 May 2004; received in revised form 1 July 2004; accepted 2 July 2004
Available online 11 September 2004

Abstract

Phenol photo-induced decomposition has been investigated in the presence of iron(III) oxide or iron(III) ions at different pH, paying particular attention to the evolution of intermediates.

The addition of halides causes a modest decrease in phenol degradation rate and starts additional transformation pathways. Chloride induces the formation of chlorinated compounds (2- and 4-chlorophenol), whose concentrations are strongly dependent on pH. Analogously, bromide ions lead to the formation of bromophenols.

Similar investigations have been performed by adopting cadmium sulfide as a photocatalyst, whose valence band edge potential (E_{VB}°) allows the oxidation of bromide but not chloride. The addition of chloride does not lead to chlorophenols, while bromide causes the formation of bromophenols, thus confirming the possibility of obtaining selective abiotic halogenation of phenol.

Keywords: Iron(III); Halophenols; Photodegradation; Cadmium sulfide; Iron oxide

1. Introduction

Semiconductors possess a particular optical band-gap that corresponds to the photon energy required to promote electrons from the valence to the conduction band [1]. The photoexcitation generates oxidative valence band holes (h_{VB}^{+}) and reductive conduction band electrons (e_{CB}^{-}). If the proper thermodynamic conditions are fulfilled, these charge carriers can react at the surface of the particles with organic and inorganic compounds [2]. The competition of interfacial charge transfers to adsorbed anions with surface OH^{-} has been investigated by time-resolved microwave conductivity [3]. EPR spectra of TiO_2 particles carrying adsorbed scavengers (e.g. inorganic anions) have suggested the formation of radical species at the TiO_2 surface.

Recently, we have observed that the addition of chloride ions inhibits the photocatalytic degradation of trichloromethane on titanium dioxide and induces tetrachloromethane formation [4]. The proposed mechanism involves the oxidation of chloride, according to reaction (1), and successive reactions of $Cl^{\bullet}$ with ${}^{\bullet}CCl_3$ (in turn originated from the competitive reaction of $CHCl_3$ with h_{VB}^{+} or trapped ${}^{\bullet}OH$).

$$h_{VB}^{+} \equiv Ti^{IV} - Cl^{-} \rightarrow \equiv Ti^{IV} - Cl^{\bullet} \quad (1)$$

These results on $CHCl_3$ prompted us to investigate the effect of chloride and bromide on the phenol phototransformation. This was done in the presence of naturally available semiconductors, in order to assess the possible formation of haloaromatics.

Pulse radiolysis studies on the kinetics and mechanism of Cl_2^{-} reaction with aromatics concluded that the direct oxidation by electron transfer is the most important reaction. The addition to the aromatic ring may also take place but at much lower rate [5]. Moreover, the study of phenol oxidative processes in the presence of TiO_2 sols, with or without chloride ions, has demonstrated the formation of phenoxy-radical mediated by Cl_2^{-} formation through valence band hole oxidation of chloride [6]. Although the primary steps seem quite different from micrometer particles of TiO_2, where chloride

---

* Corresponding author. Tel.: +39 0116707630; fax: +39 0116707615.
E-mail address: ezio.pelizzetti@unito.it (E. Pelizzetti).

1010-6030/$ – see front matter © 2004 Elsevier B.V. All rights reserved.
doi:10.1016/j.jphotochem.2004.07.003

shows an inhibitory effect, the formation of chlorine radical has received further confirmation [7–9]. Quantum yield for the formation of Cl_2^- (and the related Br_2^- and by I_2^-) on TiO_2 sols has been reported to be ca. 1% (and 5 and 11%) at 0.2 M of the corresponding sodium salt [7].

The results obtained with TiO_2 underline the possibility of achieving abiotic halogenation of aromatic rings. Here we present a similar study by using Fe_2O_3 and CdS as semiconductors. Iron oxides (for hematite the band gap equals 2.34 V, i.e. $\lambda < 530$ nm is required for photoexcitation) and cadmium sulfide ($E_{BG} = 2.4$ V, $\lambda < 517$ nm) can be activated by adsorption of ground-level solar light [10] and are widely diffused in nature, so that the photocatalytic halogenation may indicate an important natural source of halogenated compounds in the environment.

The photocatalytic properties of iron(III) oxides have been extensively investigated and it was concluded that its activity depends on the material and on the organic electron donor [11]. In the absence of suitable electron and hole scavengers at the Fe_2O_3 surface, recombination occurs within 1 ns. While oxalate [12,13] and phenol [14] were found to be successfully oxidised, other organic molecules such as citrate, benzoate and chlorinated aliphatics [11], have shown only little or no activity (quantum yield 3×10^{-8} to 5×10^{-5}). It may be questionable whether such low quantum yields are relevant to environmental processes involving the oxidation and halogenation of organic aromatics.

Cadmium sulfide possesses a band-gap requiring visible light for excitation and has been shown to photocatalytically oxidise phenol [15]. We have investigated the photoinduced transformation of phenol after halide addition to verify the possibility of obtaining selective abiotic halogenation, since E_{VB}° is able to oxidise bromide but not chloride.

The phenol phototransformations induced by Fe(III) species have also been studied. Iron(III) species under illumination in acidic media promote the photodecomposition of several organic compounds [16,17]. Photodegradation rates of triazine derivatives, for example, increase in the presence of Fe(III) salts (in concentrations of 10^{-4} to 10^{-5}M) and is dependent on the concentration of Fe(III) involved [18].

2. Experimental section

2.1. Material and reagents

The photodegradations have been performed using Fe_2O_3 (ematite, Fluka) and CdS (Aldrich) as photocatalyst. Some photodegradations have been run using $Fe(ClO_4)_3$ (Merck) as sensitizer.

Phenol (Aldrich), 2-chlorophenol (Aldrich), 4-chlorophenol (Aldrich), 2-bromophenol (Aldrich), 4-bromophenol (Aldrich) and acetonitrile (Aldrich) were used as received. Sodium chloride and potassium bromide were used after oven drying.

2.2. Irradiation procedures

The slurries were prepared by suspending in water the required amount of photocatalyst powder using sonication. Substrate aqueous solution was then added to the required amount. Experiments were run at pH 2 and 3.6, after adjustment with HNO_3, and at pH 10, obtained with addition of NaOH.

The irradiation experiments were carried out in Pyrex glass cells, containing 5 mL of the aqueous suspension of the photocatalyst powder and substrate. The illuminations were performed using a 1500 W xenon lamp (CO.FO.MEGRA, Milan, Italy) equipped with a 340 nm cut-off filter simulating AM1 solar light. The cell temperature during irradiation was 50 °C.

2.3. Analytical determinations

After irradiation the suspension was filtered through a 0.45 μm filter membrane. The disappearance of the primary compound was followed using an HPLC system (Merck-Hitachi L-6200 pumps), equipped with a Rheodyne injector, a RP C18 column (Lichrochart, Merck, 12.5 cm × 0.4 cm, 5 μm packing) and a UV–vis detector (Merck-Hitachi L-4200). The disappearance of phenol is followed at 210 nm, using an eluant composed by 40% acetonitrile and 60% phosphate buffer (1×10^{-2} M) at pH 2.8 at a flow rate of 1 mL/min.

The formation of intermediates has been followed using MS spectrometer detector (Agilent 5973) interfaced with a GC (Agilent 6890, serie II) equipped with a 5% phenylmethylpolysiloxane column (Agilent HP-5; 30 m × 0.25 mm).

The GC operating parameters were as follows: injector at 300 °C, splitless injection (1 min) and volume injected 1 μl. The analysis was performed using a double gradient. Temperature was linearly increased at 10 °C/min from 50 to 250 °C and then was brought to 300 °C at a rate of 20 °C/min.

The samples for the GC-MS analysis were extracted using dichloromethane.

3. Results and discussion

3.1. Photoassisted processes on Fe_2O_3

The photocatalytic decomposition of phenol and formation of intermediates have been studied by adopting Fe_2O_3 as a photocatalyst under different pH conditions, in the presence or absence of halides; the calculated rates of disappearance are summarised in Table 1, while the profiles for intermediates evolution are presented in Fig. 1.

Some halides (chloride and bromide) can be oxidised by valence band holes, thus acting as hole scavengers, as shown by reaction (1). The reaction steps involved in one-electron oxidation of halides (X) lead to a fast formation of an adsorbed $X^{\bullet}$ radical, followed by $X^{\bullet}{}_2^-$ radical formation

Table 1
Rate of disappearance of phenol (2×10^{-4}M) on Fe_2O_3 alone, with 0.01M NaCl or 0.01M KBr at different pH

$M \times 10^5\ h^{-1}$	Fe_2O_3	$Fe_2O_3 + Cl^-$ (0.01M)	$Fe_2O_3 + Br^-$ (0.01M)
pH 3.6	0.672	0.608	–
pH 7	0.186	–	0.089
pH 10	0.152	–	0.102

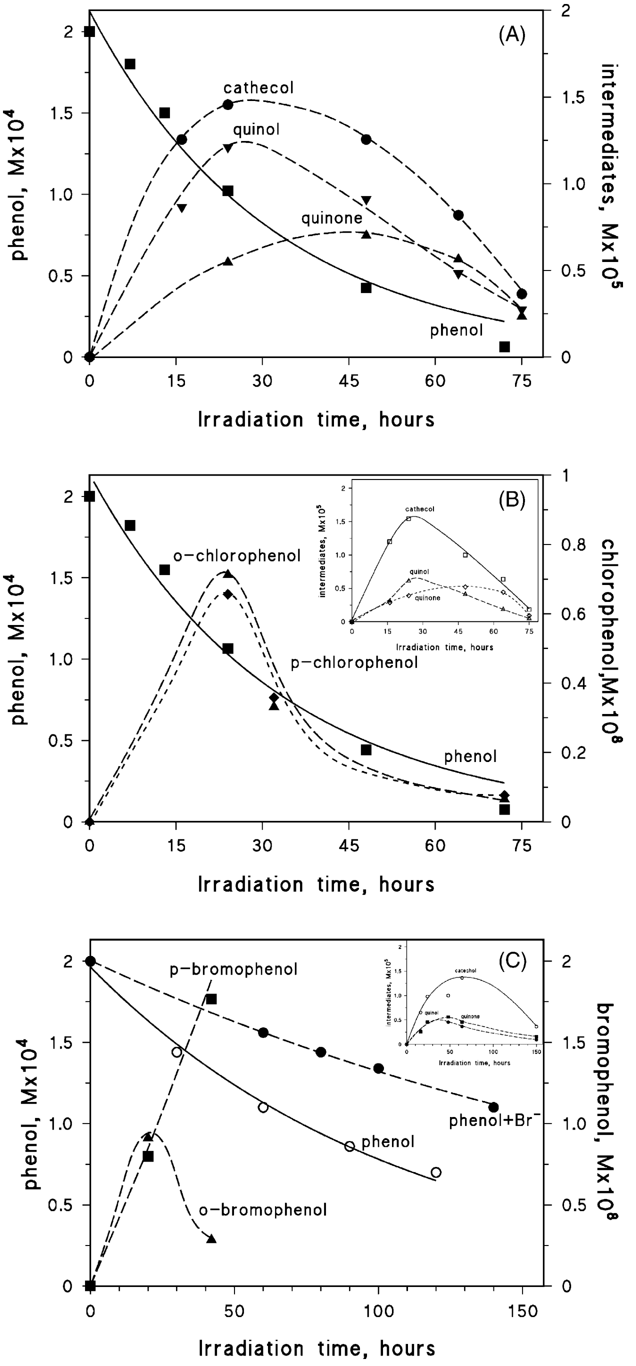

Fig. 1. Photocatalytic degradation of phenol (2×10^{-4}M) and time evolution of halophenols and hydroxyphenols in presence of Fe_2O_3 (100 mg L^{-1}); (A) without added salt at pH 3.6, (B) in presence of 0.01M NaCl at pH 3.6, (C) in presence of 0.01M KBr at pH 7.

through the reaction with $X^{-\bullet}$. However, unlike the oxyalkyl radicals, the formed radical could back-react with electrons, according to reaction (2):

$$e_{CB}{}^- + X^\bullet \rightarrow X^- \tag{2}$$

Electron recapture by adsorbed $X^\bullet$ and $X^\bullet{}_2{}^-$ follows the same mechanism.

Halide addition modifies the degradation behaviour of phenol (Table 1) showing a diminished rate of disappearance in all the considered cases. However, at pH 3.6 the presence of Cl^- ions causes only a slight inhibition ($t_{1/2}$ increases from 23 to 24 h), in agreement with other photocatalytic processes [4,10,19,20], while the main differences are linked to the evolution of intermediates. In addition to the formation of the same intermediates observed from phenol photodegradation alone (cathecol, quinol and quinone, Fig. 1A), also the formation of 2- and 4-chlorophenol is noted (Fig. 1B). Cathecol, quinol and quinone still represent the main intermediates, being formed at yields 1000 times higher than chlorophenols.

Since the $E_{VB}{}^\circ$ potential for Fe_2O_3 is 2.8 V, the generation of surficial adsorbed $^\bullet OH$ radicals and the consequent hydroxyphenols formation is allowed [14]. The oxidation of chloride could also occur according to reaction (1), being E° = 2.5 V for $Cl^-/^\bullet Cl$ and 2.3 V for $Cl_2{}^-/Cl^-$ [21], and should justify the chlorophenol formation. $^\bullet Cl$ radical is a chlorinating agent, while $Cl^\bullet{}_2{}^-$ acts as an electron transfer agent (addition rate of $Cl^\bullet{}_2{}^-$ to aromatic ring is relatively slow, $<10^7\ L\ mol^{-1}\ s^{-1}$). $^\bullet Cl$ radical is 60 times more reactive than $Cl^\bullet{}_2{}^-$. Similarly to the hydroxylation process, chlorination of phenol is regioselective too (*ortho* and *para* orientation).

In the present experimental conditions (pH 3.6) we are below the pH_{PZC} of the semiconductor (pH 8.6), so that the iron oxide surface is positively charged and chloride adsorption on the semiconductor particles is electrostatically favoured. The adsorption of Cl^- on Fe_2O_3 and the competitive oxidation of chloride ion to chloride radical lead to a decrease in the phenol rate of disappearance; the formation of chlorinated derivatives is in accordance with such observation.

Similarly, Br^- addition causes a slight decrease in phenol degradation rate and the formation of hydroxyphenols at similar yields (see Fig. 1B and C). Nevertheless, bromophenol formation is favoured, 2- and 4-bromophenol being formed at concentrations 60 times higher than the corresponding chlorophenols. This is in agreement with the redox potential of bromide couples, E° = 2.0 V for $^\bullet Br/Br^-$ and 1.6 V for $Br_2{}^-/Br^-$, so that both species may easily be formed.

At pH 7 the degradation rate of phenol is markedly decreased ($t_{1/2} \sim 70$ h) and the concentration of the formed intermediates are lowered (Fig. 1C). Bromide addition causes a further inhibition to the degradation rate (diminished by a factor 2). Brominated intermediates are formed at concentrations 20 times lower than in the experiments performed at pH 3.6.

At pH 10, even if the degradation rate is only slightly decreased, bromoderivatives formation is strongly diminished (2- and 4-bromophenol have been detected at trace level).

This inhibition in bromophenol formation may be mainly linked to:

(i) the electrostatic exclusion of bromide ions at the negatively charged particle surface;
(ii) the reduction in the driving force.

When semiconductor oxides are concerned, valence and conduction band edges potential follow a Nerstian behaviour with the pH [22,23]. Since $E_{VB}^{\circ} = 2.8\,V$, at pH 10 $E_{VB}^{\circ} = 2.2\,V$; it may be at the limit for oxidation of Cl^- to $Cl_2^{\bullet -}$, while it can still oxidise Br^- to $Br^{\bullet}/Br_2^{\bullet -}$.

The presented data suggest that chloride and bromide can compete with the organics for the oxidative holes through a direct electron transfer mechanism, since the trapped carriers (e.g. adsorbed $^{\bullet}OH$ for oxides) possess a much lower oxidation potential than the valence band hole (in the case of TiO_2 ca. 1.5 V [24]), preventing halogen radical formation.

3.2. *Photoassisted processes in the presence of iron(III)*

Different Fe(III) species co-exist in aqueous solution, whose distribution is governed by the hydrolysis equilibria shown in reactions 3–6:

$$Fe^{3+} + H_2O \rightarrow Fe(OH)^{2+} + H^+ \tag{3}$$

$$Fe^{3+} + 2H_2O \rightarrow Fe(OH)_2{}^{+} + 2H^+ \tag{4}$$

$$2Fe^{3+} + 2H_2O \rightarrow Fe_2(OH)_2{}^{4+} + 2H^+ \tag{5}$$

$$Fe^{3+} + 3H_2O \rightarrow Fe(OH)_2 + 3H^+ \tag{6}$$

Iron(III) speciation is a function of pH, so that the photoinduced process can occur in homogeneous or heterogeneous phase.

Table 2 summarises the rate of disappearance of the phenol in presence of iron(III) at different pH. At pH 2, iron(III) is prevalently in dissolved form so that the transformation process occurs in the homogeneous phase. Under the present conditions, monohydroxy complex $Fe(OH)^{2+}$ is the more important photoactive species [25], able to produce $^{\bullet}OH$ radicals through photochemical dissociation, according to reaction (7), with a quantum yield of 0.14 at 313 nm and 0.017 at 360 nm.

$$Fe(OH)^{2+} + h\nu \rightarrow Fe^{2+} + {}^{\bullet}OH \tag{7}$$

The rate of disappearance of 2-chlorophenol at constant Fe(III) shows a saturative profile as a function of the initial concentration of the organic compound [26]; both the presence of Cl^- and Br^- causes an inhibition in the degradation rate.

Table 2
Rate of disappearance of phenol (2×10^{-4}M) on $Fe(ClO_4)_3$ alone, with 0.01M NaCl or 0.01M KBr at different pH

$M \times 10^5\,h^{-1}$	Fe(III)	Fe(III) + Cl^- (0.01M)	Fe(III) + Br^- (0.01M)
pH 2	40.0	27.1	30.3
pH 6	1.88	1.36	0.71
pH 10	1.30	0.86	0.51

It has been established that the degradation products obtained when organic compounds are illuminated in the presence of Fe(III) are similar to those achieved through a Fenton's reaction, in which the $^{\bullet}OH$ species is responsible for the oxidation of organic compounds [18]. Besides reaction (7), under aerated conditions the iron(II) ions formed react with molecular oxygen to originate H_2O_2, and ultimately $^{\bullet}OH$ radicals, through reactions (8–10) [27]:

$$Fe^{2+} + O_2 \rightarrow Fe^{3+} + O_2{}^{\bullet -} \tag{8}$$

$$O_2{}^{\bullet -} + H^+ \rightarrow HO_2{}^{\bullet} \tag{9}$$

$$HO_2{}^{\bullet} + Fe^{2+} + H^+ \rightarrow H_2O_2 + Fe^{3+} \tag{10}$$

Fe(III) may also consume reductive species ($HO_2{}^{\bullet}/O_2{}^{\bullet -}$), according to reaction (11):

$$Fe^{3+} + HO_2{}^{\bullet}/O_2{}^{\bullet -} \rightarrow Fe^{2+} + O_2(+H^+) \tag{11}$$

In addition to the reactions 7–11, in presence of Cl^- reactions 12–13 could also take place [28]:

$$Fe^{3+} + Cl^- \rightarrow FeCl^{2+} \tag{12}$$

$$FeCl^{2+} + h\nu \rightarrow Fe^{2+} + Cl^{\bullet} \tag{13}$$

The simultaneous occurrence of the described steps has found support in the intermediate identification; both hydroxylated intermediates, linked to the generation of $^{\bullet}OH$ radical (through reaction 7), and halogenated intermediates, related to the formation of $^{\bullet}Cl$ radical (reaction 13), have been detected. A closer inspection of the intermediate evolutions (Fig. 2) reveals that even if halogenated intermediates are formed either in presence of Br^- or Cl^- salt, Br^- addition induces the formation of halogenated intermediates at concentrations of ca. three orders of magnitude higher than chloride. Likewise, quinone, catechol and quinol have also been identified in both cases.

At pH 6 and 10, iron(III) is prevalently present under amorphous $Fe(OH)_3$ form, and photoinduced processes should occur at the water/solid interface. Presumably the mechanism closely resembles Fe_2O_3 oxide, with surficial generation of $OH^{\bullet}/X^{\bullet}$ radicals.

The obtained profiles are reported in Fig. 3 (pH 6) and Fig. 4 (pH 10). By comparing the data at pH 2, the degradation rates are lowered 20–30 times. The diminished degradative efficiency confirms that $Fe(OH)^{2+}$ is the most active species in generating $^{\bullet}OH$ radicals, which at the present pH conditions is present in negligible amount.

At pH 6 phenol shows a half-life time of 10 h, decreased even more after the addition of Cl^- ($t_{1/2} \sim 12$ h) or Br^- ($t_{1/2} \sim 20$ h). In both cases the yields of halogenated intermediates is reduced (compare Figs. 2 and 3), above all in the case of Br^- (25 times lower).

At pH 10 (Fig. 4) the degradation rate is further diminished (see Table 2); while for phenol alone $t_{1/2} \sim 11$ h, it becomes

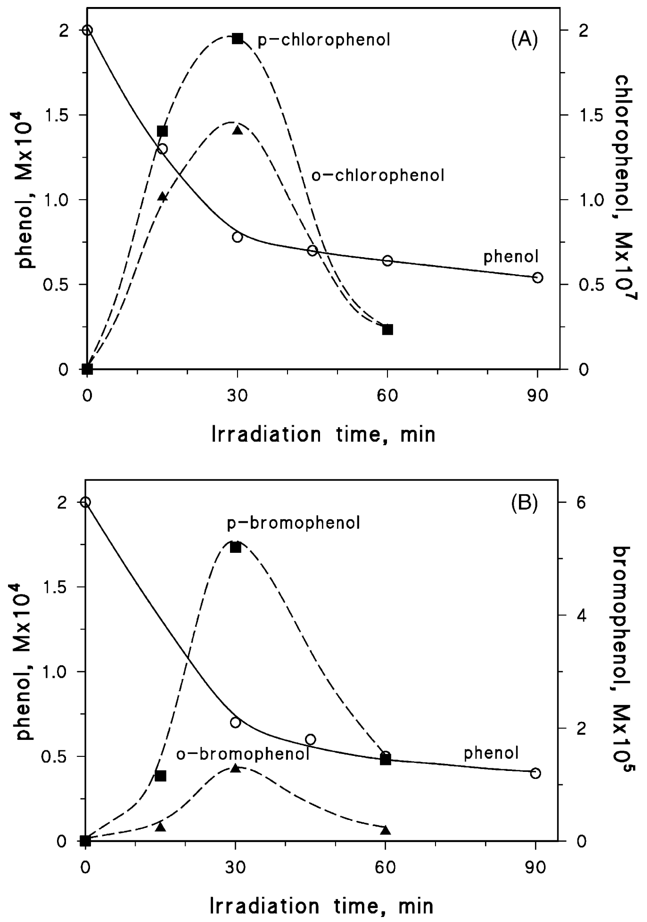

Fig. 2. Photocatalytic degradation of phenol (2×10^{-4}M) and time evolution of halophenols in presence of Fe(III) (100 mg L^{-1}) at pH 2; (A) in presence of 0.01M NaCl, (B) in presence of 0.01M KBr.

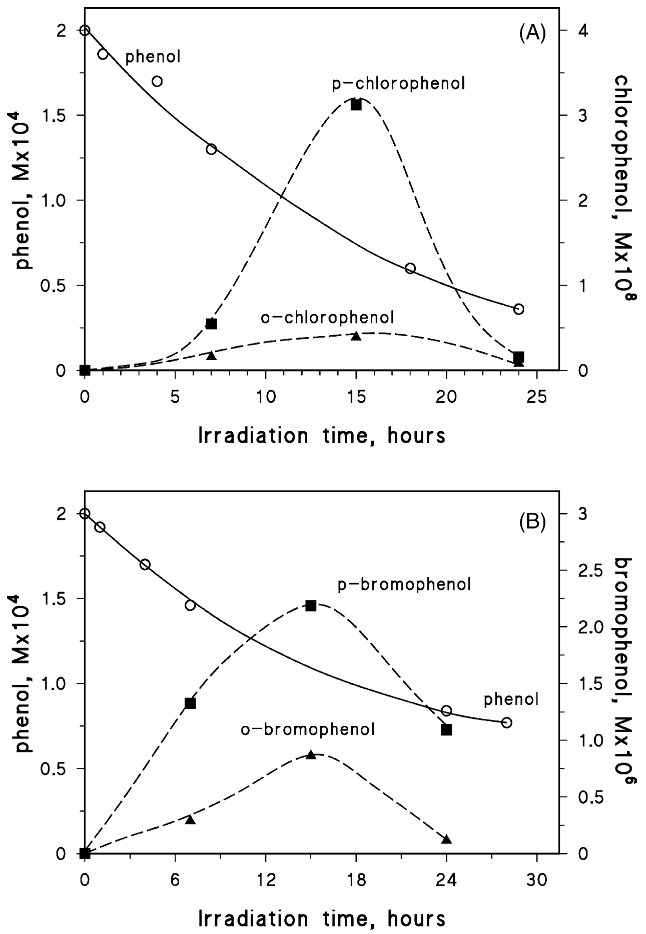

Fig. 3. Photocatalytic degradation of phenol (2×10^{-4}M) and time evolution of halophenols in presence of $Fe(OH)_3$ (100 mg L^{-1}) at pH 6; (A) in presence of 0.01M NaCl, (B) in presence of 0.01M KBr.

15 h after the addition of Cl^- ions and it is further increased with Br^- ($t_{1/2}$ 30 h). Fig. 4 also shows the formation of halogenated intermediates. *o*- and *p*-halophenol formation is strongly inhibited, particularly for the chlorophenols formed at trace level (2 ng L^{-1}). Again, the electrostatic repulsion between the surface and the halogen anion and the decrease in the thermodynamic driving force could explain the pH effect.

3.2.1. Mechanism of phenol transformation in presence of iron(III) species

The data presented above can be rationalised within the framework of the mechanism proposed in Scheme 1, which accounts for the phenol transformation products observed with Fe(III) species and iron(III) oxide. On the left side, the different Fe^{3+} aqueous species and their interactions with halides are reported, while on the right side the possible degradation steps and the supposed intermediates are summarised.

Three concomitant and competitive pathways could be distinguished, whose extent is dependent on pH conditions and on added halide. Iron(III), directly or indirectly, generates Fe(II) and $^{\bullet}OH/^{\bullet}X$ radicals. Hydroxyl radical rapidly reacts with phenol through dihydroxy cyclohexadienyl radical, which is then transformed into *ortho*- and *para*-dihydroxyphenols.

The $X^{\bullet}$ radical, in equilibrium with $X^{\bullet}{}_2{}^{-}$ radical (less reactive), can react with phenol and originate the halo-substituted phenol through the formation of a hydroxyhalocyclohexadienyl radical.

When the photoprocess occurs in presence of iron oxides, the photoactivation generates electron and holes as active species. The photogenerated electrons may react with oxygen to give a superoxide radical, while the positive holes can generate adsorbed $^{\bullet}OH$ radicals and/or $X^{\bullet}$radical. Similarly to what was discussed for the iron(III), these radicals react with phenol to give the hydroxy- and halosubstituted compounds.

3.3. Photoassisted processes on CdS

The phenol photoinduced degradation has been performed at pH 2.6 by adopting CdS as a photocatalyst, alone or in the presence of halide ions. The use of CdS suspensions in several

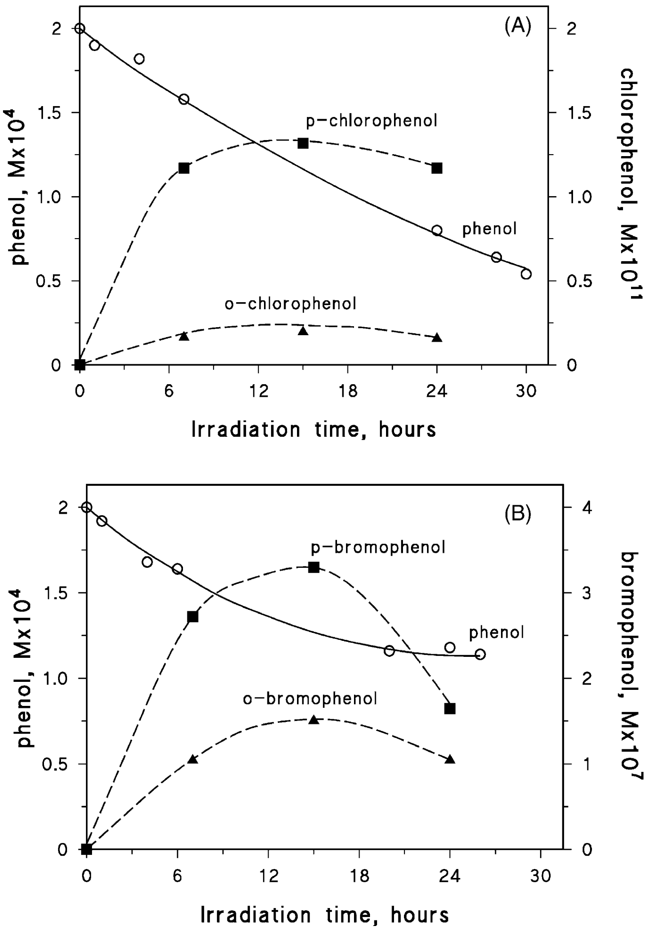

Fig. 4. Photodegradation of phenol (2×10^{-4}M) and time evolution of halophenols in presence of Fe(OH)$_3$ (100 mg L^{-1}) at pH 10; (A) in presence of 0.01M NaCl, (B) in presence of 0.01M KBr.

photocatalytic reactions has been previously investigated by White et al. [29]; the ability to oxidise phenol has been shown and confirmed under our conditions.

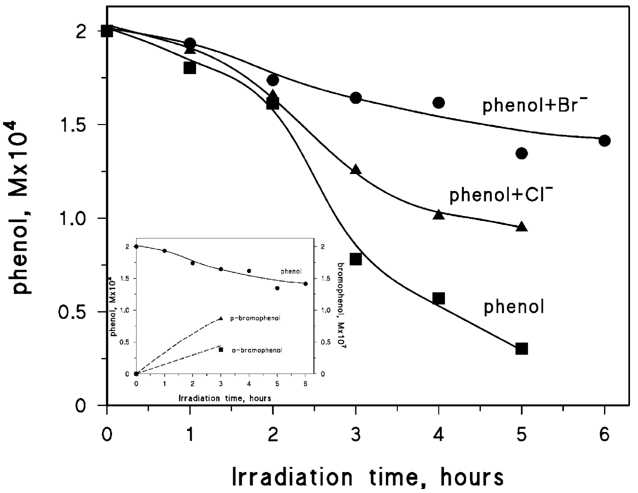

Fig. 5. Photodegradation of phenol (2×10^{-4}M) in presence of CdS (100 mg L^{-1}) in presence of 0.01M NaCl or 0.01M KBr at pH 2.6. Inset: time evolution of bromophenols in presence of KBr.

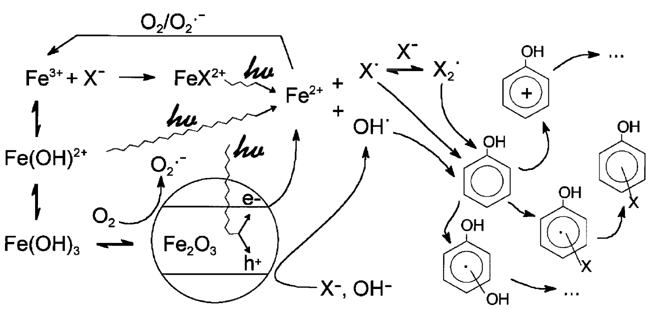

Scheme 1. Representation of the photoredox formation of chloro- and bromo-phenols in presence of iron oxide and iron(III) species/halides under illumination.

When a suspension of CdS (E_{VB}° = 2.1 V) is irradiated at pH 2.6 (dependence of flat band potential $E_{\mathrm{pH}} = E_{\mathrm{pH}_0} - 0.4$ pH) the phenol degradation alone occurs with a half-life time of 2.5 h, as shown in Fig. 5. In the present experimental conditions, the pH is below the pH$_{\mathrm{PZC}}$ (for CdS, pH$_{\mathrm{PZC}}$ 7.5 [30]), so that the catalyst surface is positively charged and it is able to adsorb halides. Similarly to what was observed when adopting Fe$_2$O$_3$, the competition between the adsorption of Cl$^-$ on CdS and the oxidation of chloride ions leads to a decrease in the degradation rate.

In the presence of phenol and chloride (0.01M), $t_{1/2}$ becomes 4 h and formation of chlorophenols is not detected [15]. The lack of chloroderivatives is thermodynamically justified; in fact, E_{VB}° is 2.0 V and the holes are not able to promote the oxidation of chloride to chlorine radical (E° = 2.6 V).

Bromide ion addition induces a further decrease in the degradation rate. Moreover, in the presence of 0.01M bromide, 2- and 4-bromophenol are formed, as shown in the inset of Fig. 5. Since E° = 2.0 V for $^{\bullet}$Br/$^{\bullet}$Br$^-$ and 1.6 V for Br$_2^{\bullet -}$/Br$^-$ [21], the oxidation of bromide ions is thermodynamically allowed. It justifies the formation of bromoderivatives and confirms the hypothesis of an abiotic photocatalytic halogenation.

4. Conclusions

Photodecomposition of phenol in presence of bromide or chloride on iron(III) oxides or iron(III) ions leads to the formation of 2- and 4-bromophenol or 2- and 4-chlorophenol. When employing CdS as a photocatalyst the formation of chloro-derivatives is not achieved, while 2- and 4-bromophenol are formed.

These results prove the possibility of obtaining abiotic halogenation of aromatic rings, so that this process should be considered as a possible abiotic source of natural halogenated organic matter. The formation of chloro- and bromoaromatics may occur under solar light in chloride- or bromide-rich environments in the presence of iron oxides or cadmium sulfide (bromoderivatives only in the latter case). These processes are relevant not only in the aquatic environments but also in atmospheric [31] and marine aerosols [32], naturally rich in chloride and bromide. The possible formation of haloorganics should also be considered in the photocatalytic purification of polluted waters.

Acknowledgements

Financial support of Ministero dell'Istruzione, Università e Ricerca through FIRB contract n° RBAU01HLFX is kindly acknowledged.

References

[1] E. Pelizzetti, C. Minero, Electrochim. Acta 38 (1993) 47.

[2] H. Gerisher, Appl. Phys. 31 (1979) 115.

[3] S.T. Mahn, H. Herrmann, M.R. Hoffmann, J. Chem. Soc. Faraday Trans. 90 (1994) 3323.

[4] C. Minero, V. Maurino, P. Calza, E. Pelizzetti, New J. Chem. 21 (1997) 841.

[5] K. Hasegawa, P. Neta, J. Phys. Chem. 82 (1978) 854.

[6] G. Gabner, G. Li, R.M. Quint, R. Quint, N. Getoff, J. Chem. Soc. Faraday Trans. 87 (1991) 1097.

[7] A. Henglein, Ber.Bunsenges. Phys. Chem. 86 (1982) 241.

[8] J. Moser, M. Gratzel, Helv. Chim. Acta 65 (1982) 1436.

[9] J.M. Hermann, P. Pichat, J. Chem. Soc. Faraday 76 (1980) 1138.

[10] R.G. Zepp, N.L. Wolfe, in: W. Stumm (Ed.), Aquatic Surface Chemistry, Wiley, New York, 1987, p. 723.

[11] C. Kormann, D.W. Bahnemann, M.R. Hoffmann, J. Photochem. Photobiol., A: Chem. 48 (1989) 161.

[12] J.M. Hermann, M.N. Morraney, P. Pichat, J. Photochem. 22 (1983) 333.

[13] J.K. Leland, A.J. Bard, J. Phys. Chem. 91 (1987) 5076.

[14] E. Pelizzetti, C. Minero, V. Maurino, Adv. Colloid Interface Sci. 32 (1990) 271.

[15] A.P. Davis, C.P. Huang, Wat. Sci. Technol. 21 (1989) 455.

[16] W. Stumm, Chemistry of the Solid-Water Interface, Wiley, New York, 1992.

[17] H. Hoignè, B.C. Faust, W.R. Haag, F.E. Sculley, R.G. Zepp, in: I.H. Suffert, P. Mac Carthy (Eds.), Aquatic Humic Substances Adv. Chem. Ser., 219, 1989, p. 363.

[18] R.A. Larson, M.B. Schlauch, K.A. Marley, J. Agric. Food Sci 39 (1991) 2057.

[19] J.C. D'Oliveira, C. Guillard, C. Maillard, P. Pichat, J. Environ. Sci. Health A: Toxic Hazardous Substance Control A28 (1993) 941.

[20] M. Abdullah, G.K.C. Low, R. Matthews, J. Phys. Chem. 94 (1990) 6820.

[21] P. Wardman, J. Phys. Chem. Ref. Data 18 (1989) 1637.

[22] E.C. Dutoit, F. Cardon, W.P. Gomes, Ber.Bunsenges. Phys. Chem. 80 (1976) 477.

[23] M. Grätzel, Fine Particles Technology, in: E. Pelizzetti (Ed.), From Micro to Nanoparticles, Lewis, Boca Raton, 1994, p. 719.

[24] D. Lawless, N. Serpone, D. Meisel, J. Phys. Chem. 95 (1991) 5166.

[25] B.C. Faust, J. Hoignè, Atmos. Environ. 24A (1990) 79.

[26] H. Kawaguchi, A. Inagaki, Chemosphere 28 (1994) 57.

[27] W. Feng, D. Nansheng, Chemosphere 41 (2000) 1137.

[28] V.A. Nadtochenko, J. Kiwi, Inorg. Chem. 37 (1998) 5233.

[29] J.R. White, A.J. Bard, J. Phys. Chem. 89 (1985) 1947.

[30] S.W. Park, C.P. Huang, J. Colloid Interface Sci. 117 (1987) 431.

[31] S.O. Pehkonen, R. Siefert, Y. Erel, S. Webb, M.R. Hoffmann, Environ. Sci. Technol. 27 (1993) 2056.

[32] R. Arimoto, W. Balsam, C. Schloesslin, Atmos. Environ. 36 (2002) 89.